Poor old pores

Rempel, Irina Lucia

Chapter 4

Replicative and chronological aging differently impact nuclear transport in baker's yeast

I.L. Rempel, L.M. Veenhoff

European Research Institute for the Biology of Ageing (ERIBA), University of Groningen, University Medical Center Groningen, 9713 AV Groningen, Netherlands

Manuscript in preparation

Keywords: nuclear transport kinetics; chronological aging; near-zero growth; water transfer; *S. cerevisiae*; microfluidics

Abstract

On the cellular level, aging is measured as the number of times a cell divides (replicative aging), or the time that a cell survives in a non-dividing state (chronological aging). Despite a few specific changes, the majority of known aging related changes are shared between both kinds of aging. Nuclear Pore Complexes (NPCs) are the conserved selective gates to the nuclear interior. They are among the largest molecular machines in cells and assembling them is a challenge. They are also long lived structures making them susceptible to accumulate damage. Previoulsy published proteomics datasets report that chronologically aged cells maintain normal FG-Nup abundance levels, while replicative aged cells lose specific FG-Nups. Here we study how nuclear transport changes in chronological aging *S. cerevisiae* cells. We show that the steady state nuclear accumulation of a GFP protein fused to a nuclear localization signal decreases during chronological aging in yeast. This is in line with previous observatios in metazoan postmitotic cells, but different from what was previously observed in replicative aging yeast cells. Altogether, our analyses show that the changes in the stoichiometry of NPC components, and the changes in transport function of the NPC are different in replicative and chronological aging yeast cells. We suggest that NPC assembly is a bottleneck for NPC function in replicative aged cells while NPC maintenance is a bottleneck for NPC function in chronolocically aged cells, and hence that aging related changes in NPCs are not shared between both kinds of aging.

Introduction

In budding yeast aging can be evaluated as the time that the cells spend in a non-dividing state (chronological aging), or the number of divisions that a cell has undergone (replicative aging). In both kinds of aging, the cell accumulates damage, which eventually causes the cell to die (Longo et al., 2012). Replicative and chronological aging are intertwined processes. Several, probably even most (Burtner et al., 2011), pathways change during both types of aging, e.g. mitochondrial dysfunction (Aerts et al., 2009; Kirchman et al., 1999), increased ROS production (Lam et al., 2011; Pan et al., 2011) and lifespan extension through dietary restriction (Goldberg et al., 2009; Lin et al., 2002) have been observed in both kinds of aging. On the other hand, both forms of aging come with distinct changes, such as accumulation of extrachromosomal rDNA circles (ERCs) in typical for replicative aging (Sinclair and Guarente, 1997).

Replicative aging has in yeast has been used as a model system to study aging of dividing cells (stem cells) in higher eukaryotic organisms, while chronological aging has been used as a model system to study aging of postmitotic cells, such as neuronal cells. The suitability of yeast as model organism to study aging is underlined by the fact that several major pathways that are implicated in aging of various higher eukaryotic model organisms are conserved and were initially discovered in aging yeast cells (Janssens and Veenhoff, 2016a). For example, the Tor/S6K pathway regulates the response to amino acid and glucose availability (Fabrizio et al., 2001) and the Ras/adenylate cyclase (AC)/PKA pathway, which also senses glucose availability, as well as other nutrients (Longo et al., 1999) were initially discovered in chronologically aging yeast cells.

Chronological aging in yeast is induced through the depletion of nurients. Commonly used protocols to achieve nutrient depletion include growing a culture to stationary phase, or transfering an exponential culture to water (Hu et al., 2013). Therefore, due to the prolongued starvation, chronological aging is characterized by upregulation of autophagy related pathways. However, prolonged starvation is a stress that postmitotic cells in higher eukaryotes do not experience and therefore, it has been suggested, to validate the results obtained from chronological aging experiments by several techniques (Hu et al., 2013; Longo et al., 2012). A more involved way to induce chronological aging, which overcomes the limitation of severe nutrient depletion in yeast, is to provide the cells with just too little nutrients to divide. Such near-zero growth experiments are performed in a retentostat (Binai et al., 2014).

Replicative aging in yeast, as well as aging in (primarily) postmitotic cells from rat brain and liver tissue samples and have been associated with changes in protein complex abundance and protein complex stoichiometry, on a proteome wide level (Janssens et al., 2015; Ori et al., 2015). One protein complex, the nuclear pore complex (NPC), was highlighted to change in various aging model systems. The NPC is one of the largest protein complexes in eukaryotic cells and mediates exchange between the nucleus and the cytoplasm, as well as assisting in various other cellular processes, most notaby gene reglation and genome stbility, discussed elswhere (Ibarra and Hetzer, 2015). NPCs act as a size dependent diffusion barrier, but they also facilitate energy dependent transport of proteins that carry a nuclear localization signal (NLS) or a nuclear export signal (NES) (Wente and Rout, 2010). Consequently changes in NPC

functionality influence the localization and function of a wide range of molecules inside the cell and has widespead effects on cell physiology.

Indeed, several studies have shown that NPCs are prone to accumulate damage and change functionality in postmitotic cells (D'Angelo et al., 2009; Ori et al., 2015; Savas et al., 2012; Toyama et al., 2013). NPCs have been studied in postmitotic cells from different tissues and different model organisms. Proteome data from aged rat liver cells were shown to have decreased numbers of NPCs in comparison to liver cells from young animals (Ori et al., 2014). Rat brain cells were shown to have carbonylated FG-Nups, decreased abundance of Nup93 (yeast Nic96) and decreased abundance of FG-domains at the nuclear envelope (D'Angelo et al., 2009). Isolated nuclei from aged *Caenorhabditis elegans* and aged rat brains were reported to be more leaky than isolated nuclei from young animals (D'Angelo et al., 2009). The scaffold of the NPC has been shown to be extremely long lived in postmitotic cells, while the FG-Nups are turned over continuously (D'Angelo et al., 2009; Savas et al., 2012).

However, NPCs have also been shown to change during replicative aging (Denoth-Lippuner et al., 2014; Lord et al., 2015; Shcheprova et al., 2008). In yeast, NPCs several proteins that are known to assist in NPC assembly decrease in abundance during replicative aging (Rempel et al., 2018). Additionally, replicative aged cells show signs of misassambled NPCs, as well as a decrease in the abundances of several FG-Nups (Rempel et al., 2018). Differently from studies performed in postmitotic tissues, replicative aging yeast cells showed an increase in nuclear compartmentalization during replicative aging, and no increased leakiness over the NE was observed (Rempel et al., 2018). The increase in nuclear compartmentalization is in line with a decreased number of passive permeable NPCs at the NE, that limit passive diffusion over the NE, without compromizing nuclear transport.

Thus, both in yeast replicative aging and in chronological aging worm or rat neuronal cells the NPC function is reported to change, but the specifics of the changes are distinct for these models of mitotic and postmitotic aging. At present, no comparisons have been made between NPC function in chronological and replicative aging cells of the same organisms. To fill this gap we compare existing proteome data on Nup abundances in chronological (Boender et al., 2011) and replicative aging (Janssens et al., 2015) and have studied NPC function in chronological aging yeast cells to complement the earlier functional studies in replicative aging yeast cells (Lord et al., 2015;

Rempel et al., 2018). We find that the changes in NPC function in chronological aging are indeed distinct from those observed in replicative aging and more in line with those observed in other postmitotic cells (rat and worm) (D'Angelo et al., 2009; Savas et al., 2012). Our work highlights that the challenges to maintian NPC function are different for chronological and replicative aging.

Results

Replicative and chronological aging show distinct changes in FG-Nup abundance during aging

Replicative aging is associated with NPC assembly problems (Rempel et al., 2018) and decreased abundance of several FG-Nups (Nup2, Nup60, Nup1, Nsp1, Nup100, Nup116, Nup49 and Nup53) on the whole cell level and at the NE (Nup2, Nup100, Nup49, Nup116) (Janssens et al., 2015; Lord et al., 2015; Rempel et al., 2018). We asked, whether a decreased abundance of FG-Nups is also found in chronologically aging cells. To address this question, we compared NPC protein abundance from two published proteome datasets, one obtained from replicative aged cells (Janssens et al., 2015) and another one obtained from chronologically aged cells, under near-zero growth conditions (Binai et al., 2014).

Since chronological and replicative aging are measured in different units (time vs. number of divisions), the most suitable way to compare the abundance of the Nups is by aligning the studies based on population viability. A viability of approximately 60% is reached after 21 days of chronological aging in near-zero growth conditions (Boender et al., 2009). We compare this condition to replicative aging after 45.4 hours of replicative aging, when an average population age of approximately 19 divisions and a viability of 77% is reached (Janssens et al., 2015). Also, indicated in Figure 1 is the abundance of the Nups after 72 hours of replicative aging, the latest timepoint in the replicative aging study and a time point where the population viability reached as low as 55 %.

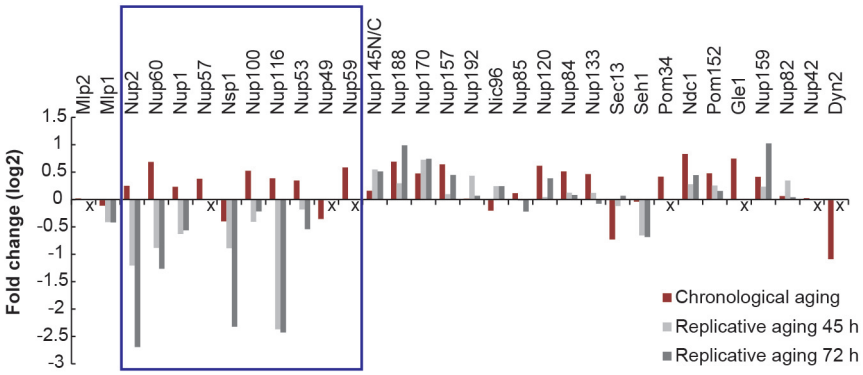

Figure 1 Distinct changes in FG-Nup abundance in replicative and chronological aging. The NPC protein abundance of chronologically aged cells, under near-zero growth conditions (Binai et al., 2014) is compared to the NPC protein abundance of replicative aged cells at two different time points. The first time point represents an age of 45.4 h and approximately 19 divisions. The second time point represents an age of 72.5 h and approximately 24 divisions; note that the spread in replicative ages in the population is very large at later timepoints due to differences in division times between cells (Janssens et al., 2015). The blue box highlights the group of nuclear and central FG-Nups. Several of those Nups show a significant decrease in abundance during replicative aging. The replicative aging proteome does not include information on the abundance of Mlp2, Nup57, Nup49, Nup59, Gle1, Nup42 and Dyn2, represented by an x on the x-axes.

The comparison between the two datasets shows that the majority of non FG-Nups, as well at the cytoplasmic FG-Nup, Nup159, show similar changes in abundance during replicative and chronological aging (Figure 1). It should be noted, that the proteins that show the most pronounced decrease in abundance during chronological aging do not uniquely function at the nuclear pore complex (Dyn2 and Sec13). The decrease in abundance of Sec13 during chronological aging is possibly related Sec13's role in CopII coated vesicle transport, which is required for cell cycle progression and cytokinesis. Dyn2 also acts as microtubule motor protein that is required for cell division. Therefore it is likely that these proteins are downregulated in non-dividing cells. The strong loss of nuclear and central FG-Nups at the whole cell level is specific to replicative aging. Chronologically aged cells show no decrease in FG-Nup abundance relative to the scaffold Nups, with the exception of Nsp1 and Nup49.

Expression of GFP reporter proteins in chronological aging

Since chronological aging can be induced by different means of nutrient starvation, we explored which chronological aging method would be suitable

for studying the localization GFP based reporter proteins, under a galactose inducible promotor. GFP based reporter proteins are small enough to passively diffuse over the NPC and have, except for the nuclear transport receptors that bind NLS or NES signals, no interactions partners that could bias their localization by retention mechanisms. Consequently, a GFP-NLS reporter protein requires constant transport in order to maintain its target localization, the nucleus. Given that the proteins are mobile, that is, not aggregated or bound in either nuclear or cytosolic compartment, one can interpret the N/C ratio's in terms of rate constant for nuclear entry and exit over the NPC.

For our studies we used GFP and a GFP-NLS reporter protein, which has a classical NLS that recruits the importins Kap60 and Kap95. For the purpose of outlining the nucleus, we used a strain expressing Nup49-mCh fusion as a marker for the NE. We tested several conditions to induce the expression of those reporter proteins in chronological aging cells. It was previously described, that the signal of a protein expressed under an galactose inducible promoter disappeared when cell cultures were grown to saturation in galactose rich medium (Cohen et al., 2016). Hence, we induced chronological aging by transferring an exponential cell culture to water. We tried to induce the expression of reporter proteins, in cells that were aged in water for several days, by adding galactose (final concentration of 0.5 %) to a small sample of the aging culture. Subsequently we quantified the localization of the reporter proteins at three different time points (1 h, 2.25 h and 3.5 h) after induction (Figure 2a). The localization of the reporter proteins was quantified by measuring the average fluorescence intensity in the nucleus and divide this value by the average fluorescence intensity in the cytoplasm (N/C ratio).

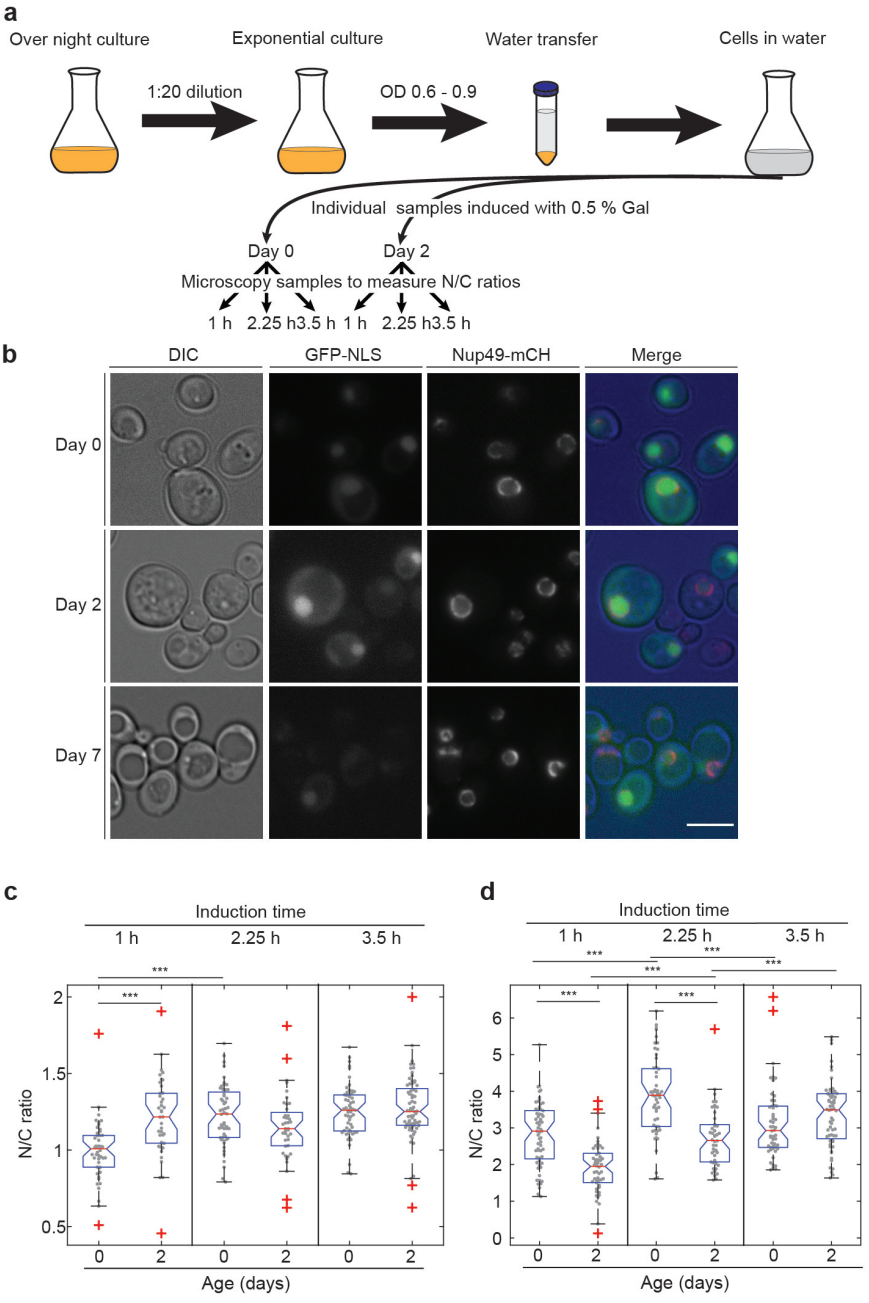
a
Over night culture
Exponential culture
Water transfer
Cells in water
1:20 dilution
OD 0.6 - 0.9
Individual samples induced with 0.5 % Gal
Day 0
Day 2
Microscopy samples to measure N/C ratios
1 h 2.25 h 3.5 h 1 h 2.25 h 3.5 h
b
DIC
GFP-NLS
Nup49-mCH
Merge
Day 0
Day 2
Day 7
c
Induction time
1 h
2.25 h
3.5 h
N/C ratio
Age (days)
d
Induction time
1 h
2.25 h
3.5 h
N/C ratio
Age (days)

Figure 2 Expession and localization of GFP-NLS reporter proteins in chronologically aged cells.
a) Schematic overview of the experimental setup.
b) Representative images of cells expressing a GFP-NLS reporter protein, after 2.25 h of induction. In the merged image, Nup49-mCh is in red and GFP-NLS is in green, and both fluorescent signals are adjusted for maximum visibility. The scale bar represents 5 μm.
c) Quantification of the localization of GFP, 0 and 2 days after water transfer, at three different time points after induction for both ages, respectively.
d) same as c but now for GFP-NLS. At least 40 cells, coming from one experiment were analyzed per sample. Significant changes in N/C ratios are indicated based on p-values <0.05, obtained from a two-tailed Student's T-test, with p-values <0.05 shown as *, p-values <0.01 shown as ** and p-values <0.001 shown as ***.

We find under this experimental condition, that only a small fraction of cells at the age of 7 days was still able to express the reporter proteins (Figure 2b). Therefore, we compared the expression of reporter proteins shortly after water transfer, with cells aged for 2 days in water. These data are to be considered preliminary as a replicate is missing, but preliminary we conclude that GFP is relatively evenly distributed between nucleus and cytoplasm and that prolonged starvation, at this early time point of chronological aging (namely 2 days) increases the N/C ratio of GFP slightly in old cells at 1 h after induction (Figure 2c). The N/C ratio of GFP-NLS increases significantly between 1 hour and 2.25 hours of induction. Furthermore, at those time points, cells that aged 2 days in water had significantly lower N/C ratios than young cells in water, possibly indicating a decrease in nucleocytoplasmic transport. After 3.5 hours of induction, the N/C ratios of young and aged cells were similar again. This could indicate, that the cells take longer to establish a steady state localization of the GFP-NLS reporter protein, but alterative explanations can certainly not be ruled out. A complication of this experimental setup is that the induction of the proteins is done using the sugar galactose, thus interfering with the chronological aging regime based on starvation.

Decreased steady state localization of GFP-NLS during chronological aging
To work around the complication of the first assay where the response to galactose addition at different chronological ages of the cells could affect the measurements, we tested another experimental setup. Here, the expression of reporter proteins was induced from a Gal1 promotor at early exponential phase. When the induced cell culture reached mid- to late exponential phase, the cells were transferred to water, which represented the start of the aging experiment. From this water culture a small sample was taken every day to quantify the localization of GFP-NLS.

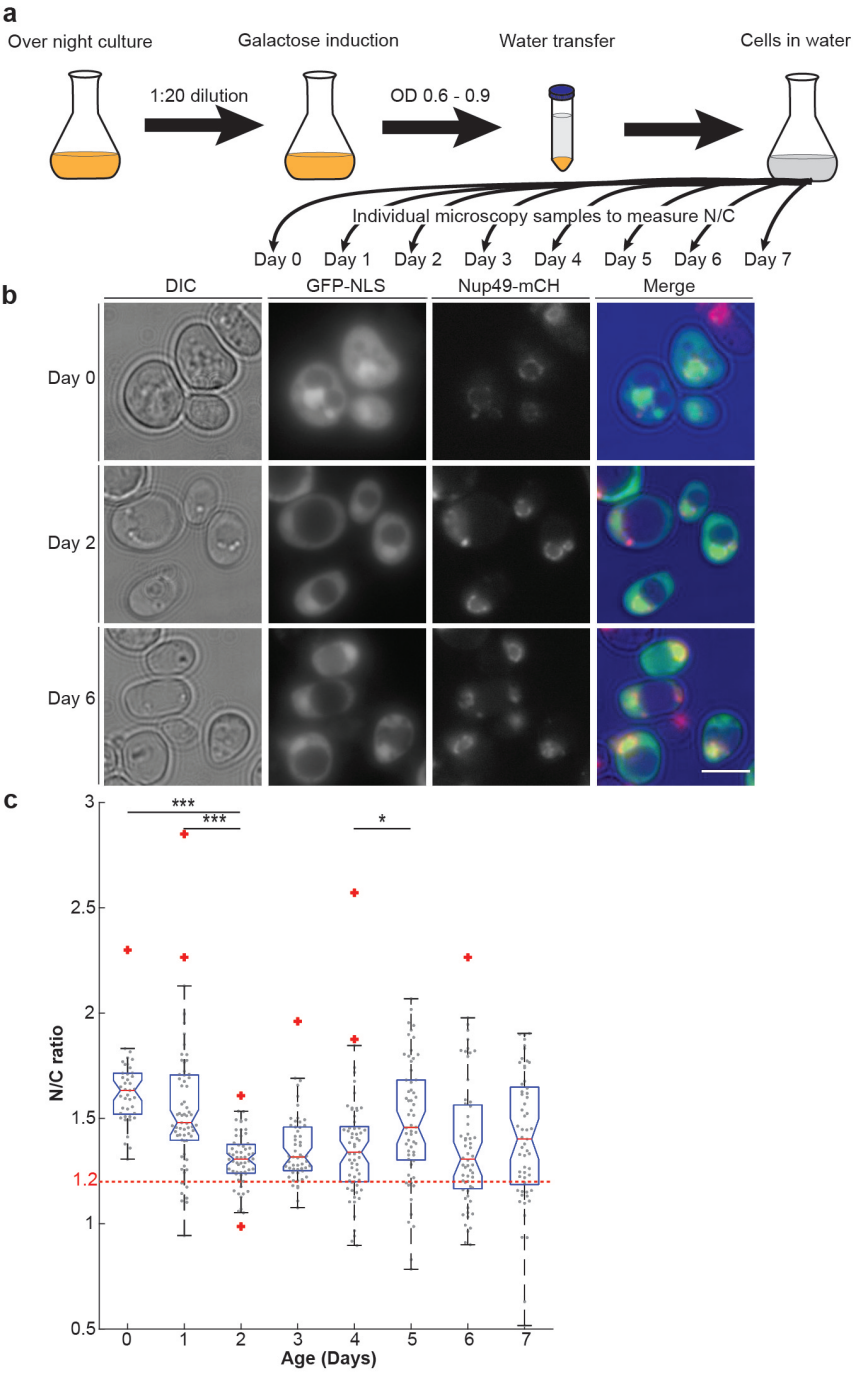
a
Over night culture
Galactose induction
Water transfer
Cells in water
1:20 dilution
OD 0.6 - 0.9
Individual microscopy samples to measure N/C
Day 0
Day 1
Day 2
Day 3
Day 4
Day 5
Day 6
Day 7
b
DIC
GFP-NLS
Nup49-mCH
Merge
Day 0
Day 2
Day 6
c
N/C ratio
Age (Days)
***
***
*
3
2.5
2
1.5
1.2
1
0.5
0
1
2
3
4
5
6
7

Figure 3 Decreased nuclear localization of GFP-NLS in chronological aged cells in water.
a) Schematic overview of the experimental setup
b) Representative images of chronologically aged cells. In the merge image, Nup49-mCh is in red, GFP-NLS is in green. The GFP and mCherry fluorescent signals in the merge image are adjusted for maximum visibility. The scale bar represents 5 μm.
c) The N/C ratio is the average fluorescence in the nucleus, divided by the average fluorescence in the cytoplasm. The nucleus is identified by Nup49-mCh which marks the NE. The line of each box indicates the median, and the bottom and top edges of the box indicate the 25th and 75th percentiles, respectively. The whiskers extend to the most extreme data points not considered outliers, and the outliers are plotted individually. Non-overlapping notches indicate that the samples are different with 95% confidence. Significant changes in N/C ratios are indicated based on p-values <0.05, obtained from a two-tailed Student's T-test, with p-values <0.05 shown as *, p-values <0.01 shown as ** and p-values <0.001 shown as ***. The dotted red line at 1.2 indicates the N/C ratio that has been previously observed for GFP and represents no accumulation (Rempel et al., submitted) (Timney et al., 2016; Webster et al., 2016).

The median N/C ratio of GFP-NLS decreases significantly from an average of 1.6 to 1.3 during the first two days, and after this initial decrease, the N/C ratio does not change significantly anymore (Figure 2a). The data presented reflect a single experiment and the increase in N/C ratio between day 4 and day 5 is unlikely to be relevant. From day one and onwards, a subpopulation of cells has lost the accumulation of GFP-NLS reporter. From day two onwards, the size of this subpopulation of cells appears to be relatively stable. We stopped analysing the N/C ratio of cells after 7 days for two reasons. The Nup49-mCh NE marker showed significant mislocalization in a large fraction of the cells and this made it difficult to identify the nucleus in an unbiased way. Additionally, the fluorescence intensity of GFP-NLS decreased prohibiting reliable quantification of N/C ratios in many cells. However, even if not quantifiable a low level of nuclear accumulation is maintained even after 7 days. Taken together, after an initial drop in the N/C ratio during the first two days, a low level of nuclear accumulation of GFP-NLS was maintained during prolonged starvation in the majority of cells, even after seven days of chronological aging.

To test if the measured N/C ratio's reflect the steady state resulting from the dynamics of import and efflux, rather that retention, we performed a so-called poison assay on chronologically aged cells. This assay uses sodium azide and 2-D-deoxy-glucose, which rapidly depletes the cellular ATP and GTP pool and hence dissipates the RanGTP/RanGDP gradient over the nuclear envelope. Consequently, GFP-NLS that is initially accumulated in the nucleus rapidly equilibrates between nucleus and cytoplasm upon addition of the poisons (Figure 4a). This equilibration between nucleus and cytoplasm should follow an exponential decay function that is asymptotic towards a value between 1 and 1.2, when GFP-NLS is not accumulated in the nucleus anymore (Meinema et

al., 2013; Schwoebel et al., 2002; Shulga et al., 1996). We excluded cells if the curve fits obtained from the single cells did not show a significant correlation to an exponential decay function or that had a low coefficient of determination (R^2) (plots lacking the red curve fit in Figure 4a and 4b). While 12 out of 14 young cells (1.5 hours after water transfer) showed loss of GFP-NLS accumulation after treatment with poison, fulfilling the given criteria for our curve fits (Figure 4a), only three out of 12 analysed cells still showed significant loss of GFP-NLS nuclear localization after seven days chronological aging (Figure 4b). This suggested, that either the majority of chronologically aged cells were, for some reason, insensitive to the poison assay, or, that GFP-NLS was immobilized in nuclei of chronologically aged cells.

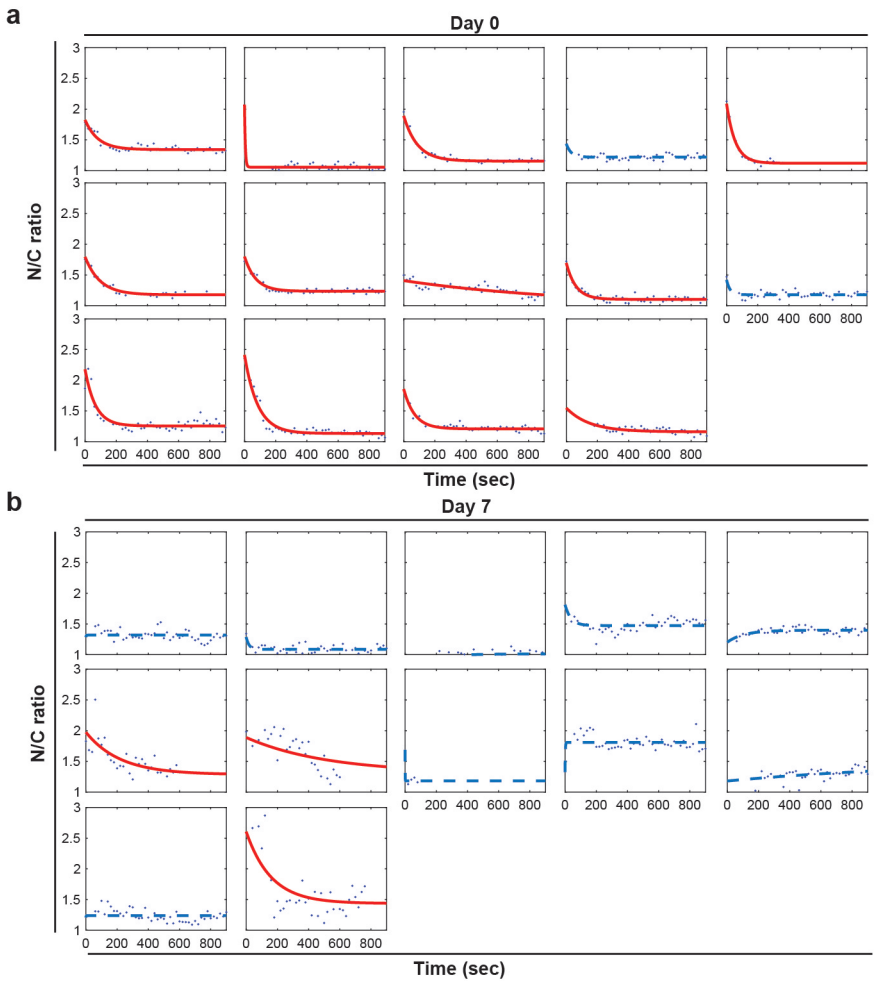

Figure 4 Chronological aged cells maintain nuclear accumulation GFP-NLS after addition of metabolic poisons (Na-azide and 2-deoxyglucose). Each plot represents one individual cell, individual N/C ratio measurements are shown as blue dots, informative curve fits are shown in red or blue; at t=0 Na-azide and 2-deoxyglcose are added. Red lines represent curve fits that fulfil the following criteria: (1) the fit has correct direction, which shows loss of nuclear accumulation, (2) The fit has a p-value <0.05 and (3) the R^2 is >0.7. Blue curves fail one or several of these criteria.
a) Leak of GFP NLS after treatment with poison for cells incubated in water for 1.5 h.
b) Leak of GFP-NLS after treatment with poison after 1 week of chronological aging in water.

As the poison assay was inconclusive with respect to answering if GFP-NLS is mobile between the cytosol and nucleus in chronological aged cells, we performed a Fluorescent Recovery after Photobleaching (FRAP) assay. For this assay we selected cells with visible nuclear accumulation of GFP-NLS and selectively bleached the nucleus of those cells. This caused an immediate drop

in N/C ratio, followed by a recovery of the N/C ratio in time. Immediately after bleaching a cell's nucleus, there is a temporary net import of fluorescent molecules from the cytosol and efflux of bleached molecules from the nucleus resulting in an increase in the N/C ratio, before fluorescent and non-fluorescent molecules equilibrate between nucleus and cytoplasm. This assay showed, that GFP-NLS was still mobile inside chronologically aged cells and that the localization of GFP-NLS still depended on energy dependent transport.

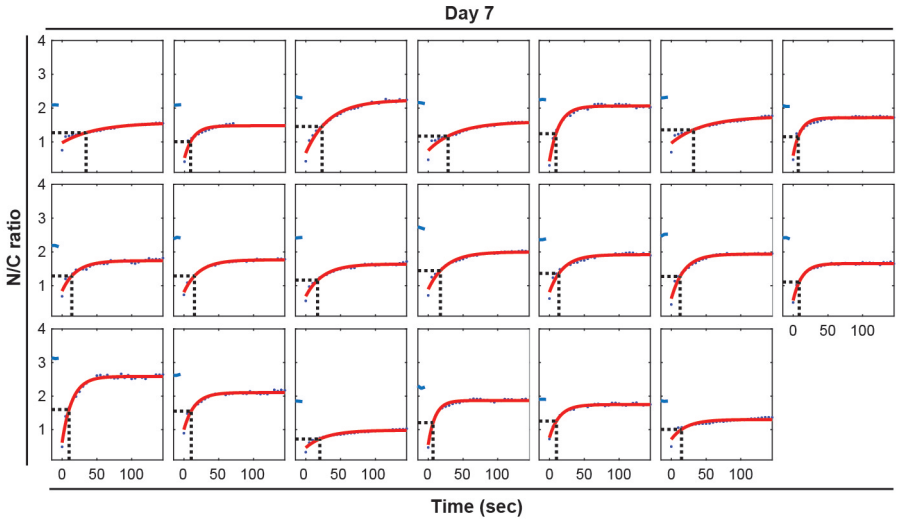

Figure 5 Nuclear accumulation of GFP-NLS in chronologically aged cells is the result of energy dependent transport. Performing FRAP experiments on chronologically aged cells, aged 7 days. Each plot represents one individual cell, individual N/C ratio measurements are shown as blue dots, curve fits are in red and the dotted lines represents the recovery half time.

Discussion

Several recent studies have shown that the NPC changes during aging, however, the changes found in replicative aged yeast cells were distinct from those found in postmitotic cells in higher eukaryotic organisms. Our previous study in replicative aging yeast cells showed increased nuclear compartmentalization and a reduction in transport dynamics across the NE (Rempel et al., 2018), while postmitotic cells show a decrease in nuclear compartmentalization and an increase in passive permeability over the NE (D'Angelo et al., 2009). We asked whether these differences were caused by the model system (budding yeast versus rats/worms), or the whether the changes were specific to the kind of aging (replicative versus chronological). Therefore, we addressed NPC related changes in transport function in chronologically aging yeast cells,

complementing previous studies in yeast replicative aging (Janssens et al., 2015; Lord et al., 2015; Rempel et al., 2018). Also we compared the loss of stoichiometry of Nups in both types of aging as measured in proteome data (Binai et al., 2014; Janssens et al., 2015).

The comparison between replicative aged yeast cells and yeast cells at near-zero growth rate showed that the loss of FG-Nup abundance is unique for replicative aged yeast cells. We consider it unlikely, that the observed differences are mainly caused by differences in the genetic backgrounds of the yeast strains used in this study, as loss of FG-Nups has been described to be present during replicative aging in three different genetic backgrounds (Janssens et al., 2015; Lord et al., 2015; Rempel et al., 2018). Replicative aging is associated with problems in NPC assembly (Rempel et al., submitted). It is unlikely that NPC assembly poses a major challenge in chronologically aging yeast cells, because several studies suggest that the scaffold of the NPC is extremely long-lived and postmitotic cells are able to survive if NPC assembly is compromised by the depletion of essential Nups (D'Angelo et al., 2009; Savas et al., 2012). The fact the loss of FG-Nup abundance is not part of the chronological aging signature supports the hypothesis that the loss of FG-Nups in replicative aging is related to NPC assembly problems.

Furthermore, we show that the steady state nuclear accumulation of a GFP-NLS reporter protein decreases during chronological aging in yeast. This change is distinct from the change in steady state localization of GFP-NLS during replicative aging of yeast, where the steady state nuclear accumulation of GFP-NLS increases during aging. The decrease in nuclear accumulation of GFP-NLS during chronological aging can have various causes, which should be addressed in future studies. Causes directly related to the transport activity over the nuclear pore complex would be (i) a decrease in the RanGTP/RanGDP gradient, (ii) an increase in passive permeability of NPCs, or (iii) a decrease in abundance of one or both of the transport factors that mediate transport of the GFP-NLS reporter molecules (Kap60 and Kap95). A more extensive FRAP study, with a larger sample size and a control population of young cells could enable us to quantify the transport kinetics of energy dependent import and of passive diffusion over the NE separately and therefore help to identify the cause for the observed decrease in steady state nuclear accumulation of GFP-NLS (import or passive diffusion). Non-NPC related changes that could influence the steady state localization of molecules are (iv) changes in the ratio of nuclear volume to cytoplasmic volume, which can impact the N/C ratio. In this case, the N/C ratio

would decrease when the cytosolic volume increase in aging relative to the nuclear volume. Additionally, (v) the compartment specific degradation of GFP-NLS reporter proteins could cause the loss of the NLS signal.

Chronologically aging yeast cells experience nutrient depletion and one must thus be careful to interpret these responses as general chronological aging responses. I.e. the decrease in steady state localization of GFP-NLS is most pronounced during the first days of the aging experiment and might be a response to prolonged starvation, rather than aging. In this case, the RanGTP/RanGDP gradient might be affected in the cells, since the gradient is dependent on the availability of free ATP and GTP in the cell. Indeed, we see in our experiments, that a fraction of the cells becomes unresponsive to the poison assay, which stops the synthesis of ATP and depletes the availability of free cellular GTP. The reason why the cells are unresponsive to the poison assay is not entirely clear, but a likely explanation is that under conditions of caloric restriction during stationary phase cellular respiration decreases (Ocampo et al., 2012) making cells unresponsive to poison, as sodium azide inhibits the final enzyme in the mitochondrial electron transport chain (Schwoebel et al., 2002).

In conclusion, we could show that changes at the NPC are distinct in replicative and chronological aging, but further studies are needed to identify the cause for the decrease in N/C ratio of GFP-NLS during chronological aging. However, an increase in passive permeability during chronological aging would explain the changes in GFP-NLS localization and would be in line with a study in higher eukaryotes which showed that NPCs are more permeable in isolated nuclei from aged rat brain and aged *C. elegans* samples (D'Angelo et al., 2009). We conclude that increased passive permeability is a possibly conserved phenotype of chronological aging. We propose, that the maintenance of long-lived protein complexes, such as the NPC, might be a general challenge to chronologically aging cells, while the assembly of long-lived protein complexes might be a general challenge in replicative aging cells.

Materials and methods

Strains, plasmids, and growth conditions

Experiments in this study were performed with *S. cerevisiae* cells from BY4741 genetic backgrounds. Cells were grown at 30°C, shaking at 300 RPM using Synthetic complete medium supplemented with 2% D-glucose or 2 % D-raffinose, unless indicated otherwise. All reporter proteins were expressed under

the *Gal1* promoter. 0.5 % or 4 % D-galactose was used for induction of reporter proteins. Cells were induced for 4-7 h prior to the start of an experiment.

yPP008; GFP-NLS Nup49-mCh (*MATa his3Δ1 leu2Δ0 met15Δ0 ura3Δ0* GFP-tcNLS(pGal1)::His Nup49-mCh::URA)	Rempel et al., 2018

Chronological aging experiments

Different chronological aging protocols were tested. (1) (Cohen et al., 2016) tried to age cells in medium and induce the expression of GFP-NLS in exponential phase, and then grow the culture to saturation. (2) We grew a cell culture to saturation and took a small sample at several time points and then induced expression of reporter proteins for up to four hours prior to microscopy. (3) We transferred an exponential cell culture to water, aged the cells and took small samples each day, in which we induced the expression of reporter proteins with a final concentration 0.5% D-galactose. Microscopy samples were taken 1 h, 2.25 h and 3.5 h post induction. (4) As described in (Cohen et al., 2016), cells were inoculated into SD-complete medium, supplemented with 2% Glucose grown over night. The next day, cells were diluted in Sgal-complete medium supplemented with 4% D-galactose and grown to an OD_{600} between 0.6 and 1. Then cells were harvested and resuspended in water. The cells were kept in water shaking at 30°C. From this chronologically aging culture, small samples were taken every day for a total of one week.

Poison assay inside the microfluidic chip

ALCATRAS 1 (Crane et al., 2014) was used to measure the age dependency of passive permeability of the NPC during chronological aging. Fluorescent images were taken at the beginning of the experiment. To obtain passive permeability of old NPCs, the cells were aged in water for seven days. Subsequently the cells were loaded into the microfluidic chip and the medium in the chip was exchanged for glucose-free medium supplemented with 10 mM sodium azide and 10 mM 2-deoxy-D-glucose. In young cells, the presence of sodium azide and 2-deoxy-D-glucose is known to destroy the Ran-GTP/GDP gradient over the NE and abolish active transport of reporter proteins (Meinema et al., 2013; Schwoebel et al., 2002; Shulga et al., 1996). To measure the changes in reporter protein localization, we imaged the cells every 30 s during the experiment, for a total time of 15 min.

Microscopy

Microscopy was performed on a Delta Vision Deconvolution Microscope (Applied Precision), using InsightSSITM Solid State Illumination of 488 and 594 nm and an Olympus UPLS Apo 100x oil objective with 1.4NA. Detection was done with a CoolSNAP HQ2 camera for the poison assays and using a PCO-edge sCMOS camera for the FRAP assays. All experiments were performed in a temperature controlled environment at 30°C.

To ensure constant environmental conditions for the duration of the FRAP experiment, chronologically aged cells were loaded into a microfluidic chip (ALCATRAS) (Crane et al., 2014)(Rempel et al., submitted). The nuclear fluorescence was bleached using the spot laser Photokinetics module at 488 nm at 100 % for 2 ms at minimum laser spot radius. Three images were taken prior to the bleaching event. After the bleaching event, images were taken every 5 s for the duration of 150 s, during this time nuclear and cytosolic fluorescence equilibrated.

Data analysis

Microscopy data was quantified with open source software Fiji (Schindelin et al., 2012). To quantify the localization of the reporter proteins, the average fluorescence intensity at the nucleus was measured and divided by the average fluorescence intensity at the cytoplasm (N/C ratio). The significance of changes in N/C ratio were determined with a two tailed Student's t-test. Changes were significant when $p < 0.05$. The single-cell measurements obtained from poison assays and FRAP experiments were fitted to an exponential decay function in MATLAB.

Acknowledgements

This project was funded by the Netherlands Organization for Scientific Research (NOW open 824.15.020) and a gift from the Ubbo Emmius Fund to the Veenhoff lab. The FRAP assays were performed at the UMCG Imaging and Microscopy Center (UMIC), which is sponsored by NOW-grants 40-00506-98-9021(TissueFaxs) and 175-010-2009-023 (Zeiss 2p).